Turkish J. Eng. Env. Sci.
26 (2002) , 265 – 274.

Low Cycle Fatigue Properties of 2124/SiC$_p$ Al-Alloy Composites

İlyas UYGUR
University of Wales, Swansea, Department of Materials Engineering,
Singleton Park SA2 8PP, Swansea-UK
Mustafa Kemal KÜLEKCİ
Abant İzzet Baysal University, Technical Education Faculty,
14400 Düzce - TURKEY
e-mail: kkulekci@yahoo.com

Received 22.03.2001

Abstract

In this article, powder metallurgy processed metal matrix composites are tested under the strain control loading conditions. The influence of volume fraction (17 and 25 vol%), particulate size (2.5 and 15 μm) of reinforcement particles and strain ratio (R=0, R=0.5 and R= -1) are examined for 2124 Al-alloy-T4 composites. Increasing the content of SiC$_p$ results in the degradation of strain control fatigue properties. The monotonic and cyclic stress-strain response of the 2124Al – (25 vol% 2.5 μm) SiC$_p$ composite was significantly altered by strain ratio values. Fatigue cracks frequently initiated from intensively stress concentrated regions. Increasing volume fraction and particle sizes result in early crack initiation.

Key words: Composites, Fatigue, Low cycle fatigue

Introduction

Metal matrix composites (MMCs) have received significant attention due to their excellent combination of physical and mechanical properties, such as a low density, high tensile strength, enhanced stiffness, high operating temperatures, and wear and creep properties compared with conventional engineering materials (Suresh *et al.*, 1993). The fatigue behaviour of MMCs is a very important factor for many engineering applications involving cyclic or dynamic loading. It has been reported that incorporation of hard ceramic particles resulted in low crack propagation rates, especially at low ΔK levels in composite materials compared with their unreinforced counterpart (e.g., Bonnen *et al.*, 1990). However, it was found that the presence of reinforcement particles in MMCs dramatically reduces the low cycle fatigue response of composites under strain controlled cyclic loading conditions. An increased volume fraction (V_f) and particle size (P_s) of the reinforcement particles cause further reductions in low cycle fatigue responses (Srivatsan, 1992; Srivatsan, 1993; Srivatsan *et al.*, 1993). The reduction in the strain controlled fatigue response of MMCs is attributed to several factors. These include the stress concentration at the hard ceramic particles, high dislocation density near the interfaces, the brittle nature of ceramic particles, low monotonic ductility, hydrostatic stress state development and plastic flow constraint within the matrix alloy (Everett and Arsenault, 1991; Llorca, 1994; Srivatsan and Parash, 1994).

Various studies, both numerical and experimental, have been carried out for the monotonic stress-strain behaviour of particulate and whisker reinforced Al-alloy composites (Corbin and Wilkinson, 1994; Llorca *et al.*, 1991; Llorca *et al.*, 1992) as well as for the cyclic stress-strain behaviour of these composites (Llorca, 1994; Han *et al.*, 1995; Sasaki *et al.*, 1994; Srivatsan *et al.*, 1991).

The objective of this study is to discuss the strain controlled fatigue response of 2124 precipita-

tion hardened Al-alloy reinforced with SiC particulate. The efects of volume fraction (V_f) particle size (P_s) of reinforcement and strain ratio (R) are examined under strain control conditions in various strain ranges. Direct comparisons between monotonic and cyclic stress strain responses are also considered. Fatigued samples are examined using scanning electron microscopy in order to understand the failure mechanism (SEM).

Materials and Experimental Procedure

The tested materials were commercial 2124 (Al-Cu-Mg-Mn) Al-alloy with 17vol% and 25vol% with SiC particles. All of the materials, which were referred as AMC217 (17vol% 2-3 μmSiC_p), AMC225 (25vol% 2-3 μm SiC_p), LAMC217 (17vol% 10-20μm SiC_p), and LAMC225 (25vol% 10-20 μm SiC_p), were produced by Aerospace Composite Materials (UK) using powder metalurgy (P/M) processing. Mayes servo-hydraulic machines were used for strain controlled tests. Prior to the machining process a solution treatment was applied at 505 ^{o}C for 1 hour, followed by quenching into cold water. The materials were then naturally aged at room temperature for 100 hours. The alloy composition is given in Table 1. Typical micrographs of the AMC217 and AMC225 composites are shown in Figures 1a and b.

Cylindrical hourglass-shaped specimens that have 6mm diameter and 65mm long gauge sections were machined from the extruded bars. The length to diameter ratio was chosen so as to assure that specimens would not bend under compressive loading. The stress axis of fatigue was parallel to the extrusion direction. Three different strain ratios (R= -1, fully reversed, R=0.5 and R=0 zero tension) were used with a triangular waveform of loading and a strain rate of 10^{-3} s^{-1}. An axial 9mm extensometer was attached to the gauge section of the sample to check the total strains. The stress-strain ($\sigma - \varepsilon$) hysteresis loops were recorded by computer.

The fracture surfaces of the specimens after fatigue testing were examined using a JEOL 35c type scanning electron microscope at an operating voltage of 20 kV. Fatigued specimens at various strain ranges and strain ratios were selected in order to study the characteristics of the fatigue crack formation and growth.

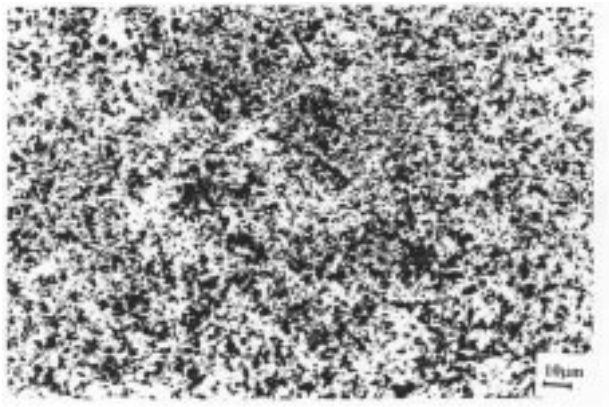

Figure 1a. Microstructure of the AMC217-T4 (17 vol % 2.6μm SiC_p) fine particulate MMC.

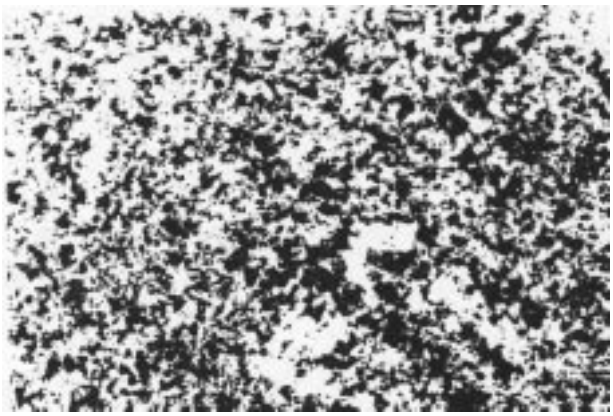

Figure 1b. Microstructure of the AMC225-T4 (25 vol % 2.4μm SiC_p) fine particulate MMC.

Results and Discussion

The effect of volume fraction and particle size on low-cycle fatigue response (LCF)

The influence of discontinuous SiC_p reinforcement on the strain controlled fatigue life response of the AMC217 and AMC225 composites can be seen in Figure 2. Cyclic strain life resistance significantly decreased when SiC_p content increased from 17vol% to 25vol% at R=0 strain ratio. The effect of the volume fraction (V_f) of reinforcement particles was marked at all strain range levels (in particular, at an equivalent strain range of 0.41 the degradation was as high as 95% in AMC225 with V_f=0.25). Limited experiments were carried out for understanding the effect of particle sizes. The particle sizes (2.5 and 15μm) did not significantly alter the strain controlled fatigue life response of MMCs at R=0 (Figure 2). However, many researchers (Srivatsan and Au-

radkar, 1992; Srivatsan and Parash, 1994; Karma *et al.*, 1998) reported that introducing the high volume fraction and coarse reinforcement size significantly reduced the LCF properties of similar composites. Similarly, fatigue lives of circular cylindrical specimens under the strain control are shown in Figure 3 in terms of the R=-1 strain ratio. It was clearly observed that the fatigue life of the AMC225 was much shorter than that of the AMC217 material at the high strain range levels. However, the life difference decreases with decreasing strain range.

It is well documented that strain control fatigue data on plain laboratory specimens can be represented by the summation of elastic and plastic strain components (Manson and Hirschberg, 1964).

$$\Delta\varepsilon_t = C_p(N_f)^{\alpha_1} + C_e(N_f)^{\alpha_2} \qquad (1)$$

where $\Delta\varepsilon_t$ the total strain range, $N_f$the number of cycles, α_1 the plastic strain exponent, α_2 the elastic strain exponent, Cp the plastic strain constant and C_e the elastic strain constant at N_f=1. Typical elastic and plastic best-fit curves of the AMC225 are shown in Figure 4 and elastic and plastic coefficients of these lines are collected in Table 2 for each condition. It can be seen from Table 2 that increasing V_f and P_s significantly reduces the elastic and plastic coefficient and constant of the composites. This may suggest that the coarse SiC particles reduce the fatigue life of the composites compared to their fine particulate counterparts. This is logical because the increase of SiC_p content in matrix material will concentrate highly localized plastic deformation around the particles (Everet and Arsenault, 1991).

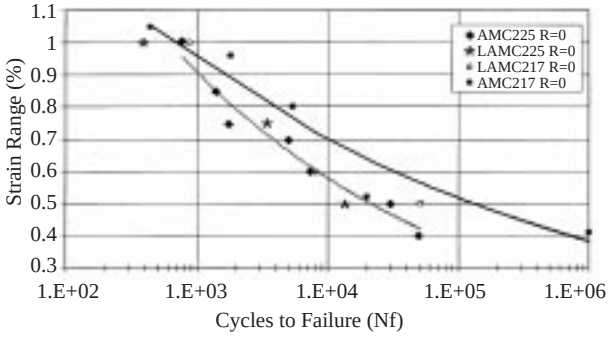

Figure 2. The effect of partical size and volume fraction of reinforcement particles on the strain controlled fatigue life response of composites at R=0 conditions.

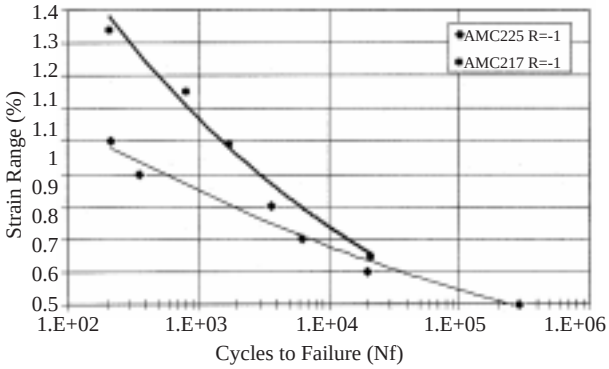

Figure 3. The effect of reinforcement volume fraction on strain controlled fatigue life response of the AMC217 and the AMC225 composite materials at R=-1 conditions.

Table 1. Chemical composition of the 2124 Al-alloy composites

Element	Cu	Mg	Mn	Fe	Si	Others	Al
Weight %	3.86	1.50	0.6	0.01 Max	0.05 Max	0.1 Max	Balance

Table 2. Coefficients to describe the strain control fatigue response of MMCs.

R ratio	Material	α_1	C_p	α_2	C_e
0	AMC217	-0.3271	0.0729	-0.0132	0.0036
0	LAMC217	-0.276	0.0565	-0.0087	0.0017
0	AMC225	-0.311	0.0553	-0.0088	0.00223
0	LAMC225	-0.16	0.02344	-0.0088	0.0018
0.5	AMC225	-0.193	0.02511	-0.00876	0.0063
-1	AMC225	-0.139	0.0199	-0.00876	0.00112

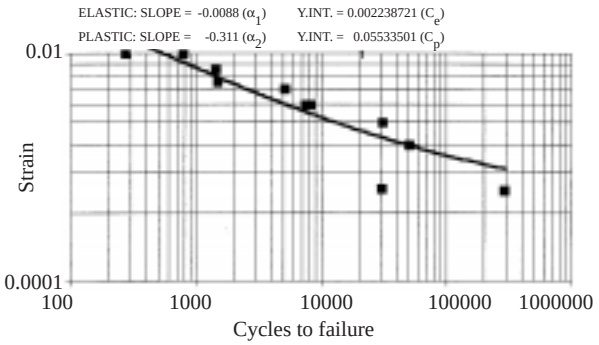

Figure 4. Elastic and plastic best fit curve of the AMC225 at R=0.

With continued cyclic straining, many microcracks would initiate over the poles of SiC_p and rapidly link to form a macroscopic crack. The propagation of these cracks will be faster than that of the fine particulate and low volume fraction composites (Sasaki *et al.*, 1994). Moreover, comparison of the LCF properties of base Al-alloys and composites revealed that, base materials had a significantly superior life response at the same strain amplitudes than composites. This was attributed to the low monotonic ductility of the composites, stress concentration, high dislocation density at interfaces, residual stresses which induce the particle fracture and debonding (Han *et al.*, 1995; Li and Ellyin, 1996; Llorca, 1994). Hence, an increase in V_f and P_s will reduce the tensile ductility of composites, and also reduce the LCF properties. A primary factor contributing to these lower life times was related to the concentration of plastic strains. Although the composites were deformed to an equivalent average plastic strain, considerably higher local plastic strains were subjected over the pole of the SiC_p. Thus, a higher degree of fatigue damage was induced in these locations than would be anticipated from the average plastic strain inside the composite material (Suresh *et al.*, 1993).

The cyclic stress-strain response of MMCs is illustrated in Figure 5 at the first cycle and R=0 strain ratio. The first cycle increasing V_f of reinforcement SiC particles increased the hyteresis loops of the stress responses of MMCs. However, the presence of coarse reinforcement particles (10-20μm) in AMC217 and AMC225 materials did not modify the first cycle stress response. There was an asymmetry in the stress response between tension and compression, which can be attributed to the influence of the thermo-residual stress distribution in the composite (Srivatsan *et al.*, 1994).

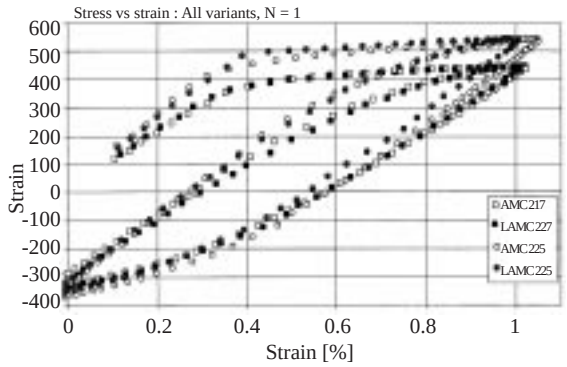

Figure 5. The first cycle stress-strain response of MMCs at R=0 and 1% strain at room temperature.

Typical maximum and minimum stresses for the number of cycles are shown in Figure 6. The compression stress response of the MMCs improves due to the increase in the reinforcement particles. Although these materials were tested under the same conditions, the increased V_f of SiC particles caused more than 50% life degradation. Also, it is clear that both tensile and compressive stresses were stabilised after a few decades of cycles. This stability was typical for all variants of composites and all different strain range levels.

The cyclic stress amplitude response during a total strain controlled fatigue test versus normalised (percentage) number of cycles (N/N_f) at a different strain range for 2124+SiC_p composites is shown in Figure 7. At all strain ranges, materials progressively hardened and occasionally softened only prior to the failure. The cyclic hardening response dominated for the fatigue lives (10-20%) and the cyclic stable behaviour dominated for fatigue lives (80-90%). The specimen subjected to higher strain ranges showed more cyclic hardening for a given condition. It is revealed that the MMC containing a high V_f and small P_s has, greater cyclic strength and degree of hardening than others. The overall degree of cyclic hardening decreased with a decreasing $V_f$and coarse $P_s$of SiC_p reinforcements. The possible micromechanisms governing the hardening behaviour during cyclic straining may be related to a combination of the following changes in the material structure (Srivatsan and Auradkar, 1992):

(a): Load transfer between the soft ductile matrix and the hard brittle ceramic particles

(b): Presence of a pre-existing dislocation density caused by the SiC_p

(c): Presence of intermetallic particles and small precipitates

(d): Residual stresses in the MMC

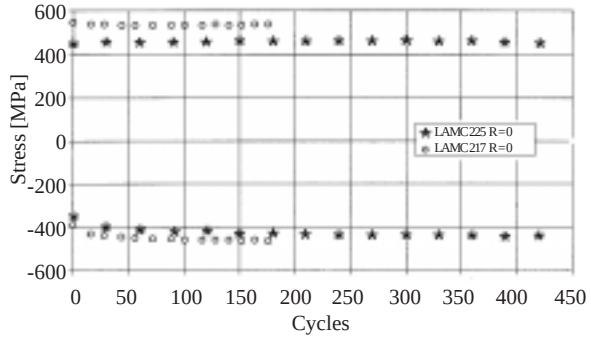

Figure 6. Typical maximum-minimum stress life response of coarse particulate MMCs at 1% strain range and R=0.

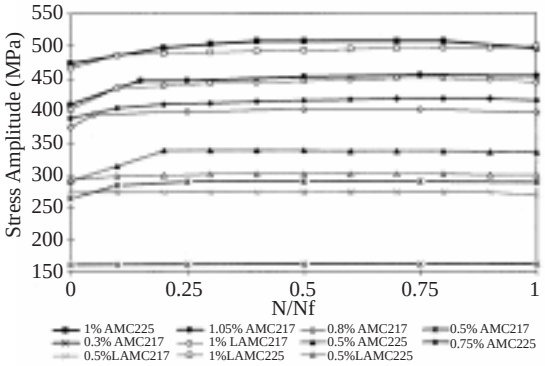

Figure 7. Comparison of the effect of cyclic total strain range on cyclic stress response of the 2124/SiC particulate reinforced MMCs with all different variants at R=0. N/N_f denotes percentage life.

However, hardening behaviour was less marked, and most of the fatigue lives saturation (stable) behaviour occurred after a few decade cycles and continued until failure in the present composite materials. This stable behaviour was assumed to be as a result of mobile dislocations which were blocked between the SiC particles and precipitates to accommodate the plastic strain without further hardening (Llorca, 1994). At very low strain ranges ($\Delta_\varepsilon = 0.4$), the elastic behaviour of the composite was linear. Thus, cyclic strain hardening or softening was not observed during the fatigue life.

The monotonic and cyclic stress-strain curves for AMC217 and LAMC217 MMCs are presented in Figure 8a. The cyclic stress response was slightly lower than monotonic stress response, and at a mid-strain ratio it did not modify the cyclic stress response of AMC217 material.

Comparison of monotonic and cyclic stress-strain behaviour of AMC225 and LAMC225 MMCs is presented in Figure 8b. Similarly, 25vol% SiC_p reinforce composites were cyclically stable compared to the monotonic response. The size of the reinforcement particles did not change this stability.

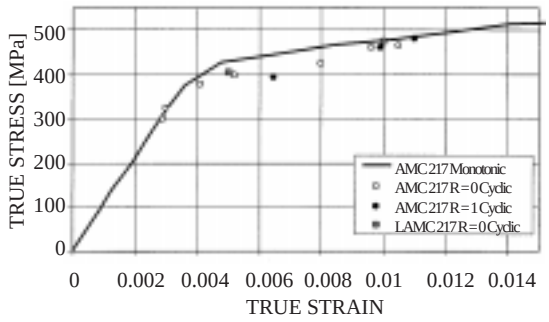

Figure 8a. Comparison of monotonic and cyclic stress-strain response of the 17vol% SiC_p composites at R=0 and R=-1 conditions.

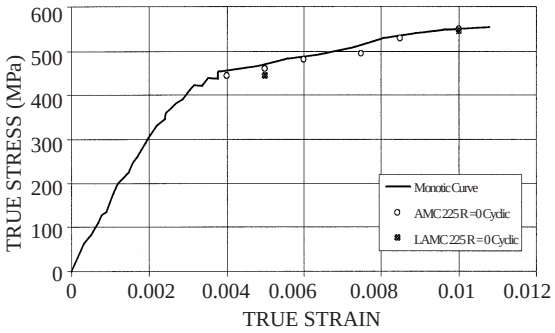

Figure 8b. Comparison of monotonic and cyclic stress-strain response of the 25vol% SiC_p composites at R=0 condition.

The effects of strain ratio on LCF

The strain control fatigue response of AMC225 (2124+25 vol% 2-3μm SiC_p) material was tested using three different R ratios and various strain range levels. A typical fatigue life response of AMC225 material is shown in Figure 9. It was revealed that for the zero-tension tests, strain controlled fatigue life was slightly better than the fully reversed fatigue life response at high strain ranges. However, reduction of fatigue lives was observed at R=0 in the of low strain range levels compared with R=-1 ratio. The strain controlled life response of the composite was reduced by increasing the R ratio from R=0 to R=0.5 because of the very high amount of stress and strain response. Similar results were obtained with load controlled fatigue life response of the same material (Suresh *et al.*, 1993).

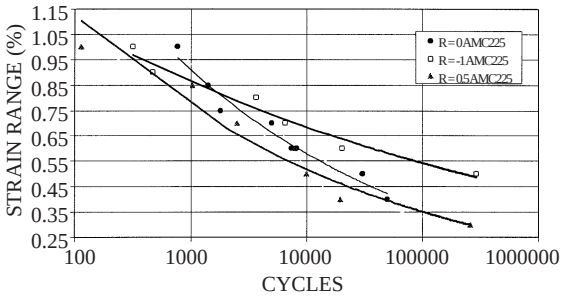

Figure 9. The influence of the three different R ratios on strain controlled fatigue life response of AMC225 material in air.

The comparison of the first hysteresis loops and stabilised loops is presented in Figures 10a-c at three different R ratios and 1% strain range level. Four different types of R ratio effect were observed in these figures:

(a): Maximum tensile stresses the were same as the stabilised loops response (N_1=N_{312}=555MPa, $\Delta_{\varepsilon t}$ = 1%). However, compressive stresses were significantly increased or hardened due to the residual stress in MMC at R=0 (N_1=-400MPa, N_{312}=-490MPa, $\Delta_{\varepsilon t}$ = 1%). The same effect of R ratio was seen at all strain range levels.

(b): The stabilised tensile and compression stresses were increased when compared with the first cycle stress response at R=-1 ratio (N_1=564MPa and –455 MPa, N_{145}=565 MPa and –490 MPa, $\Delta_{\varepsilon t}$ = 1%). Similar results were also observed at different strain ranges.

(c): Although the tensile stress response slightly decreased at stabilised loops, the compressive stress significantly increased when compared with the first cycle stress response at R=0.5 strain ratio (N_1=600MPa and –390MPa, N_{90}=595MPa and –470 MPa at $\Delta_{\varepsilon t}$ = 1%). The compressive stresses were quite low, but the tensile stresses were very high when compared with the two other R ratio levels. Very high maximum tensile stress caused a decrease in the fatigue life response.

(d): The cyclic plastic strain ranges were significantly altered by R ratios. The measured plastic strain ranges are given in Table 3. It can be seen that there were significant reductions in plastic strain ranges with increased R ratios. It is also worth noting that the cyclic plastic strains decreased in the stabilised loops while the total strain ranges were constant.

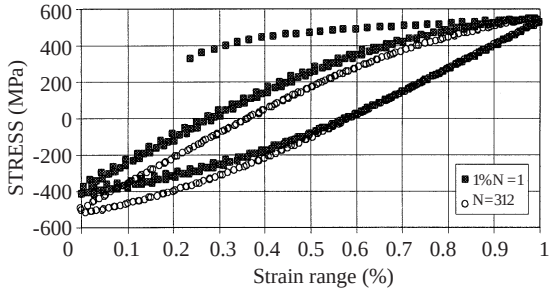

Figure 10a. First and stabilised loops stress-strain response of AMC225 at R=0 and 1% strain range.

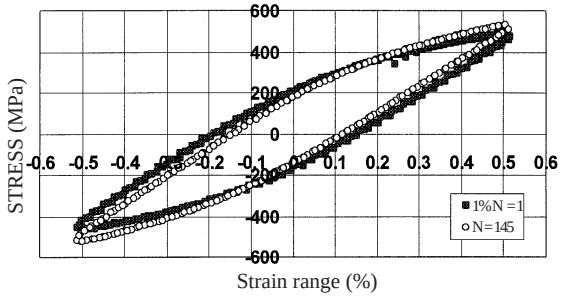

Figure 10b. First and stabilised loops stress-strain response of AMC225 material at R=-1 and 1% strain range.

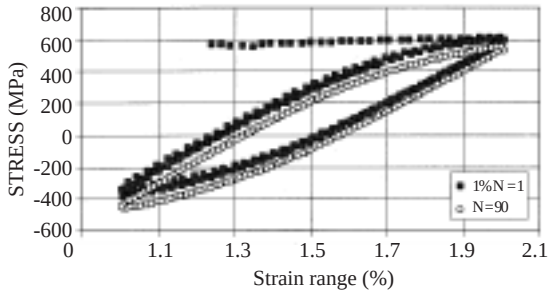

Figure 10c. First and stabilised loops stress-strain response of AMC225 material at R=0.5 and 1% strain range.

The cyclic and monotonic stress-strain response of AMC225 material is shown in Figure 11. MMC had a strain hardening regarding the R=0.5. The MMC had softened during cyclic straining at low strain ranges and at increased strain ranges. Monotonic and cyclic stress response were superimposed at R=-1. The monotonic and cyclic stress response of the material was mostly stable at R=0. These results explain that the highest stress response of AMC225 caused the least fatigue life response at R=0.5. The

Table 3. Measured plastic strains at first and stabilised loops at various total strain ranges for AMC225 MMC.

Total strain and measured cyclic plastic strains at first and stabilised cycles				
R ratios	$\Delta\varepsilon_t = 1\%$	$\Delta\varepsilon_t = 0.8 - 0.85\%$	$\Delta\varepsilon_t = 0.6\%$	$\Delta\varepsilon_t = 0.4 - 0.5\%$
0	N_1=0.54% N_{312}=0.4%	N_1=0.216% N_{800}=0.098%	N_1=0.6% N_{5680}=0.05%	N_1=0.038% N_{26600}=0.018%
-1	N_1=0.48% N_{145}=0.42%	N_1=0.25% N_{2200}=0.12%	N_1=0.093% N_{3500}=0.047%	N_1=0.024% N_{40000}=0.013%
-0.5	N_1=0.39% N_{90}=0.39%	N_1=0.146% N_{1930}=0.07%	N_1=0.051% N_{7610}=0.049%	N_1=0.0197% N_{15800}=0.019%

stabilised stress response of MMC had an average fatigue life response at R=0.5 and the cyclically softened MMC had the greatest fatigue life response at R=-1 during the strain controlled fatigue test.

The cyclic best-fit lines can be obtained through the following equation:

$$\Delta\sigma/2 = K(\varepsilon_p/2)^n \tag{2}$$

where $\Delta\sigma/2$ is the cyclic stress amplitude, K is the cyclic fatigue coefficient, $\varepsilon_p/2$ is the plastic strain amplitude and n is the cyclic hardening exponent. The resultant coefficients are given in Table 4. It can be seen that both values were increased. The effect of R ratios with respect to the Coffin-Manson relationship is presented in Table 2. The cyclic stress-strain responses of AMC217 and IMI834 materials were extensively discussed by Bache *et al.*, (1995).

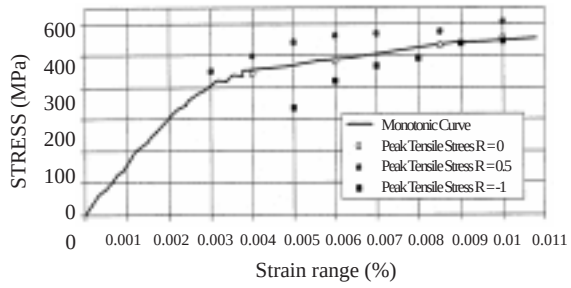

Figure 11. Comparison of cyclic and monotonic stress-strain response of AMC225 MMC material with different strain ratios under the strain controlled fatigue conditions.

Fracture surface studies

Examination of the strain controlled fatigue fracture surfaces of the deformed plain specimens in the SEM were carried out at low magnification to identify the overall fracture and fatigue initiation and at the high magnification to describe the fatigue fracture mode and particle matrix interaction. Representative fractography of the fracture surface features at low magnification is shown in Figure 12. On a macroscopic scale, the fracture surfaces were found to vary with SiC_pcontent in the 2124 matrix. An increased reinforcement volume fraction and particle size caused more brittle and flat fracture surfaces. All fracture surfaces were roughly 90^o to the applied stress axis. River-like patterns from the nucleation region can be seen in Figure 2. At high magnification, examination of nucleation sites revealed that crack initiation emerged by the following features under strain controlled fatigue conditions: (a): Copper-rich intermetallic large particles around 40μm (Figure 13). (b): Large SiC particles as big as 25μm. (c): Extremely large SiO_2 particles as big as 300 μm. (d): Indistinguishable initiation, suggesting that the nucleation arises from the secondary machining process.

For a similar volume fraction and particle sizes of SiC_p reinforced fracture surface revealed very similar topographies at high intermediate and low cyclic strain ranges at all different strain ratios. However, at high magnification, fracture surfaces were found to vary with reinforcement content and sizes. Four characteristics were observed in the study of fracture surfaces at high magnification.

Table 4. Coefficients to describe plastic cyclic stress-strain curves for AMC225 material at different R ratios.

R ratio	K	n	Strain Range
-1	1801	0.2	0.004 – 0.01
0	1945	0.224	0.005 – 0.01
0.5	2245	0.243	0.003 – 0.01

Figure 12. Low cycle fracture surface of AMC225 material ($\Delta\varepsilon_t$ = 1%, R=-1, N_f=235 cycles, $\sigma_{\max}$ = 530MPa, Hz triangular wave from in air)

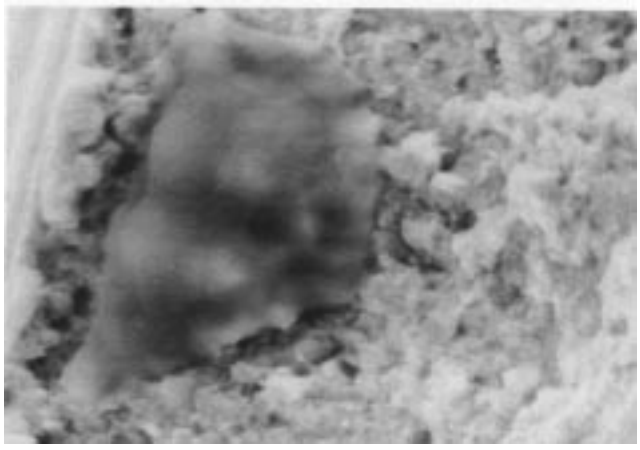

Figure 13. Copper-rich intermetallic particle, at the nucleation region of the AMC225 material at above conditions.

1. All fracture surfaces had a dimple morphology, which indicates ductile fracture mode. Most of these dimples resulted from fracture or decohesion of SiC particles.

2. There were mainly two dimple populations: the first one was related to SiC particles and increased in size as the size of the reinforcement particles were increased. The second population consisted of very small dimples ($\approx 1\mu m$) located in the space between the reinforcement particles associated with fine intermetallic particles (Figure 14).

3. The particle cracking and cleavage between $SiC_p$and matrix material became more evident as the SiC_p size and content increased (Uygur, 1999). There were a few observations of pull out of particles from the Al-matrix, which indicates quite a good interfacial bonding (Figure 15).

Figure 14. SEM picture showing coarse and fine ductile dimples on the fracture surface of AMC225 material ($\Delta\varepsilon_t$=0.4%, R=-1, N_f=50000 cycles,$\sigma_{\max}$=440 MPa, 1 Hz triangular wave form in air)

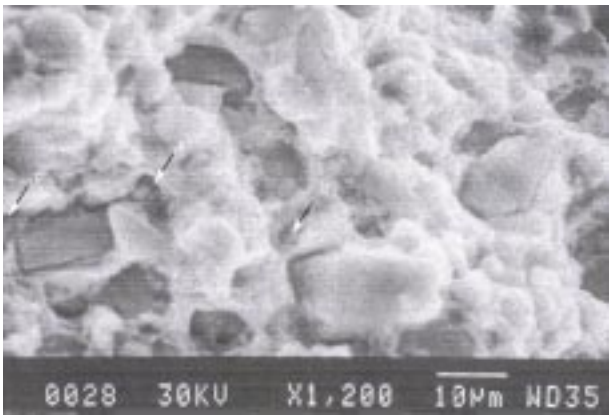

a). Pull out. b). Small dimples. c). Particle cracking and cleavage.

Figure 15. High magnification SEM picture showing particle cracking cleavage between SiC particle and matrix material on fracture surface of the LAMC217 material at R=0, ($\Delta\varepsilon_t$=1% in air.

4. The larger SiC particles tend to crack or cleave during cyclic deformation while the finer particles tend to decohere from the matrix to produce ductile dimples. Overall fracture surfaces clearly indicated that the cyclic deformation properties of Al-alloy matrix were significantly altered by the presence of reinforcement particles (Suresh *et al.*, 1993). Therefore, increasing the content of the reinforcement particle leads to crack propagation and early crack initiation, which results in a reduction in the fatigue resistance of the materials.

Conclusions

From the results presented above, the following conclusions can be drawn:

1. Increasing volume fraction and particle size of reinforcements decreased the strain controlled fatigue life response of the composites. A higher volume fraction and finer particulate sizes of the SiC_p resulted in an increase in hardening behaviour with fatigue lives.

2. Comparison of monotonic tensile stress-strain response and cyclic maximum stress-strain response of AMC225 composite showed stabilised behaviour at R=0 strain ratio. Similar stabilised behaviour was observed at high strain levels at fully reversed (R=-1) strain ratio. However, the composite showed cyclic softening at low range levels. The composite material showed cyclic hardening at the R=0.5 condition in almost all strain levels.

3. Cyclic stress amplitude response of 2124 25% 2-3μm SiC_p-T4 Al-alloy revealed some initial hardening at almost all strain ranges. However, most of the normalised fatigue lives (80-85%) were stable until failure at room temperature under the strain controlled fatigue conditions.

4. For given volume fractions and particle sizes, fracture morphology was found to be essentially matrix dominated and similar in appearance in fracture surface for the different strain range and strain ratios in the composite materials. Fracture surfaces of the composites revealed an overall brittle appearance on a macroscopic scale. However, the presence of ductile dimples and their coalescence on a microscopic scale ensured the general fracture behaviour, which was ductile mode, caused by void nucleation. Propagation and coalescence of voids at intensive damage regions were observed (i.e. cluster of particles, coarse particles of SiC particles).

Nomenclature

R	strain ratio
ΔK	stress intensity factor
V_f	volume fraction
P_s	particle size
T_4	solution treatment + naturally aged
σ	stress
Δ K	stress intensity factor (K_{max}-K_{min})
ε	strain
$\Delta\varepsilon_t$	total strain range
N_f	tumber of cycles until failure
α_1	plastic strain exponent
α_2	elastic strain exponent
C_p	plastic strain constant at N_f= 1
C_e	plastic strain constant at N_f= 1
$\Delta\sigma/2$	cyclic stress amplitude
K	cyclic fatigue coefficient
ε_p	plastic strain amplitude
n	cyclic hardening exponent
SiC_p	SiC articulate
MMC_s	metal matrix composites
LCF	low cycle fatigue

Acknowledgements

The authors would like to thank Abant Izzet Baysal University for its financial support of the study and Prof. W.J. Evans for his valuable discussions on the subject.

References

Bache, M.R., Evans W.J., and Rees, G., "Fatigue Responce of Titanium Alloys", Proceedings of the International Conference on Air Breathing Engines, Melbourne, Australia, 61-67, 1995.

Bonnen J.J., You C.P., Allison J.E., and Jones J.W., Fatigue Properties of SiC Particulate Reinforced Al-Alloys", Proceeding of 4th International Conference on Fatigue, (ed. Kitagava, H., and Tanaka, T.), Honolulu, 887-892, 1990.

Corbin, S.F. and Wilkinson, D.S., "Low Strain Plasticity in a Particulate Metal Matrix Composite", Acta Metallurgica, 42 (4), 1319-1327, 1994.

Everett, R.K. and Arsenault, R.J., "Metal Matrix Composites: Mechanism and Properties", Acta Metallurgica, 38 (2), 712-717, 1991.

Han, N.L., Wang, Z.G. and Sun, L.Z., "Effect of Reinforcement Size on Low Cycle Fatigue Behaviour of SiC Particle Reinforced Aluminium Matrix Composites", Scripta Metallurgica et Materialia, 33(5), 781-787, 1995.

Kamat, S.V., Varma, V.K., Mahojan, Y.R., and Kutumbarao, V.V., "Cyclic Stress Response of Al-Cu-Mg Alloy Matrix Composites With SiCp of Varying Sizes", Scripta Materiale, 38 (10), 1571-1575, 1998.

Li, C. and Ellyin F., "Fatigue Crack Growth in Particle Reinforced Metal Matrix Composite", Material Science & Engineering, A214, 115, 1996.

Llorca, J., Needleman, A., and Suresh, S., "An Analysis of the Effects of Matrix Void Growth on Deformation and Ductility in Metal-Ceramic Composites", Acta, Metallurgica. 39(10), 2335, 1991.

Llorca, J., Suresh, S., and Needleman, A., "An Experimental and Numerical Study of Cyclic Deformation in Metal-Matrix Composites", Metallurgical Transaction, 23A, 919-934, 1992.

Llorca, J., "A Numerical Study of the Mechanisms of Cyclic Strain Hardening in Metal-Ceramic Composites", Acta Metallurgica. 42(1), 151, 1994.

Manson, S.S., and Hirschberg, M.H., Fatigue: An Interdisciplinary Approach, Syracuse University, New York, 1964.

Sasaki, M., Lawson, L., and Meshii, M., "Low-Cycle Fatigue Properties of a SiC Whisker-Reinforced 2124 Aluminium Alloy", Metallurgical and Materials Transaction, 25A, 2265-2274, 1994.

Srivatsan, T.S., Parash, A., "The High Strain Cyclic Fatigue and Fracture Behaviour of 2090 Aluminium Alloy", Engineering Fracture Mechanics, 40(2), 297-309, 1991.

Srivatsan, T.S., and Auradkar, R., "Effect of Silicon Carbide Particulate on Cyclic Plastic Strain Response Characteristic and Fracture of Aluminium Alloy Composites", International Journal of Fatigue, 14(6), 355-366, 1992.

Srivatsan, T.S., Lanning, D., and Soni, K.K., "Cyclic Strain Resistance and Cyclic Fracture Behaviour of 2124 Aluminium Alloy", International Journal of Fatigue, 15(3), 231-242, 1993.

Srivatsan, T.S., Parash, A., "Effect of Particulate Silicon Carbide on Cyclic Strain Resistance and Fracture Behaviour of X2080 Aluminium Alloy Metal Matrix Composites", Engineering Fracture Mechanics, 49(5), 751-772, 1994.

Suresh, S., Mortensen, A., and Neddleman, A., Fundamentals of MMCs, Butterworth- Heinemann Publishing Company, Stoneham, USA, 1993.

Uygur, İ., "Environmentally Assisted Fatigue Response of Al-Cu-Mg-Mn With SiC Particulate Metal Matrix Composites.", PhD Thesis, University of Wales, Swansea, UK. 1999.